Emergent magnetism from lithium freezing in lithium-doped boron nitride

Adam Berlie,[1,2,*] John W. White,[3] Mark Henderson,[4] and Stephen Cottrell[1]

[1]*ISIS Neutron and Muon Source, Science and Technology Facilities Council, Rutherford Appleton Laboratory, Didcot, OX11 0QX, United Kingdom*

[2]*RIKEN Nishina Centre for Accelerator-Based Science, 2-1 Hirosawa, Wako, Saitama 351-0198, Japan*

[3]*Research School of Chemistry, The Australian National University, Canberra, 2601, Australia*

[4]*State Key Laboratory Cultivation Base for Nonmetal Composites and Functional Materials, Southwest University of Science and Technology, Mianyang 621010, China*

(Received 24 April 2017; published 10 October 2017)

The synthesis and characterization of Li-doped boron nitride is reported where the sample is in the dilute limit with a stoichiometry of $Li_{0.01}(BN)_3$. The diffusion of atomic Li dominates above 150 K, with $D_{Li} \sim 10^{-10}$ cm^{2}s^{-1}, where the Li diffusion rate increases with temperature resulting in activated behavior with an energy scale of 27 meV. Below 150 K the Li diffusion freezes out and the sample enters a magnetic state at approximately 70 K that shows evidence for being glassy in nature. It is believed that this is due to the freezing of Li atoms within the lattice which then involves partial electron injection into the BN layers, and this provides a mechanism for magnetic exchange, resulting in a divergence of the magnetic susceptibility. Our work shows the promise of this material for future study, where there is currently much interest in Li base compounds for energy storage.

DOI: 10.1103/PhysRevMaterials.1.054405

I. INTRODUCTION

There is a large amount of interest in lithium based compounds for applications in batteries as well as other energy materials. In these systems one generally relies on the diffusion of Li ions, rather than atomic Li, to create a current with the aim of having a high capability, a high charge capacity, and, for cathodes, a high voltage [1]. Here we study lightly doped lithium boron nitride so we can compare the properties with graphitic intercalation compounds (GICs). These have well documented temperature dependent phase changes [2] which highlight their potential for hydrogen storage [3–5]. GICs also have interesting magnetic and superconducting properties as well as being used in battery materials [6]. Although LiC_6 shows no superconducting properties, increasing the stoichiometry by high pressure synthesis to LiC_2 results in a T_C of 1.9 K [7], demonstrating that these systems are extremely sensitive to the amount of Li that is essentially stuffed into the layers. Since GICs have shown such promise, it is reasonable to look at other materials that may show interesting intercalation abilities and properties. Hexagonal-boron nitride (h-BN) and graphite have many similarities yet pose some stark differences. Both are isoelectronic and have a similar layered hexagonal structure. However, the electronic states are different and, unlike graphite, there is no overlap of HOMO-LUMO orbitals. As a result it has a large band gap of 4 meV. Due to differences in electronegativity between B and N, one ends up with a polarized B-N bond. Therefore, the whole system can be thought of as inhomogeneous regions of charge density that should have profound effects on the properties.

Intercalation of alkali metals into h-BN has been described [8–10]; however, it has proved hard to achieve uniform doping. Intercalation of potassium into h-BN results in a $(2 \times 2)R$ 0° structure within the BN layers [9]. Li-doped analogs have proved more difficult to synthesize but a feature is the expansion of the lattice, where the (002) peak in the XRD patterns were shifted to lower 2θ or higher d-spacing. This is also true within transition metal intercalted h-BN samples [11]. NMR of ball milled samples shows very broad peaks, where higher doping levels result in a broad peak with a decrease in chemical shift indicating a change in the interactions between the Li atoms and h-BN lattice. There has also been various computational studies to try to understand different magnetic states in h-BN [12–15] as well as hydrogen storage in the intercalated compounds, although this has been limited to computational studies [16,17]. In all cases there has been very little physical synthesis and characterization; thus many of the properties remain elusive. Our work addresses this issue of little information on the synthesis and characterization of an intercalated h-BN sample. Unexpected properties emerged from the synthesis of bulk Li intercalated h-BN and so we use a suite of techniques to understand the Li diffusion and magnetism, which include magnetic susceptibility, muon spin spectroscopy (μSR) and NMR. The use of μSR to study Li diffusion has some advantages over NMR, when paramagnetism is present. Previous work by Sugiyama *et al.* [18] on $Li_xCo_{1-x}O_3$ has shown that activation energies determined by μSR were a factor of 3 different than that from Li NMR [19] as well as having better agreement with calculated Li diffusion constants. Our work shows that as the temperature is decreased, the sample moves through two regions: one at high temperatures where the behavior is dominated by Li diffusion, and another at 150 K where an emergent magnetic state is formed as the Li atoms freeze into a disordered magnetic state.

II. EXPERIMENTAL: CHEMICAL SYNTHESIS AND PHYSICAL CHARACTERIZATION

The lithium-doped h-BN was made from commercial boron nitride powder, outgassed at 300 °C and 10^{-5} torr, transferred to a steel reactor under pure argon and reacted with stoichiometric quantity of lithium metal for $Li(h\text{-}BN)_3$ at 200 °C for 0.5 h; more information on the synthesis can be

*adam.berlie@stfc.ac.uk

found within the Supplemental Material [20]. The product was a light violet color, similar to that observed for K doped h-BN [9]. Electron spin resonance was used to estimate the number of Li atoms within the sample and a nominal stoichiometry of $Li_{0.01}(BN)_3$ was calculated using a Cu^{2+} standard. This material showed a strong Dysonian ESR line shape at 298 K associated with the absorption from conduction electrons. On cooling to 25 K a sharp line appears on top of the broad peak and on further cooling to 6 K, two sharp lines with a $g \approx 2$ arise. We attribute this to two different sites of the Li, such as bulk metallic Li and random individual Li atoms. Henceforth the sample will be referred to as LiBN. The sample was characterized using powder diffraction under argon in a sealed x-ray capillary on a PANalytical Empyrean diffractometer with focusing optics and Cu-K_α radiation with a wavelength 1.541 Å [21].

For the magnetic measurements, a sample of LiBN was sealed inside a Teflon bucket sample holder made by Quantum Design. This was then used in conjunction with the reciprocating sample option (RSO) on a Quantum Design MPMS with a 70 kG superconducting solenoid. The sample was cooled down to 10 K at two different cooling rates: 10 K/min and 2 K/min, but from 10 K to 2 K only 2 K/min could be used. Zero-field-cooled (ZFC) and field-cooled (FC) scans were then carried out in an applied field of 500 G with the temperature swept from 2 K to 300 K at a rate of 0.5 K/min.

Muon spin relaxation/rotation measurements were carried out using the EMU spectrometer [22] at the ISIS Neutron and Muon Source, United Kingdom. The sample was loaded inside an argon glovebox and sealed inside a titanium sample can with a thin titanium foil window. A helium exchange cryostat was used to control the temperature with an accessible range of 1.5 K to 300 K. The technique, known commonly as μSR, involves implanting an ensemble of spin polarized positive muons into a sample; the muon spin precesses around any internal local magnetic field. If the internal field is homogeneously distributed, you have a coherent precession of the muon spin where $\omega = \gamma_\mu B$, B is the applied field, γ_μ is the gyromagentic ratio of the muon and ω is the precession frequency of the muon spin. As the internal field distribution broadens, the muon ensemble polarization dephases and the decay is measured. In all cases the muon rotation or relaxation is observed by measuring the asymmetry of the muon decay into positrons, where the positron is emitted preferentially along the direction of the muon spin, using a forward and backward detector bank. The current work uses both zero-field (ZF) and transverse field (TF) μSR to characterize the Li diffusion and magnetism within the material. Complementary wideband ^{7}Li ($\gamma_{Li}/2\pi = 16.547$ MHz/T, $I = 3/2$) NMR measurements were conducted using a Bruker Avance machine with a frequency of 700 MHz with the sample sealed inside a quartz tube. The frequency used for the experiment was 272.13207 MHz with a LiCl standard using a reference at 298 K.

III. RESULTS AND DISCUSSION

Intercalation involves transfer of electron density from the lithium atom into the BN ring structure, creating a local magnetic moment and a partial charge on the 2D BN

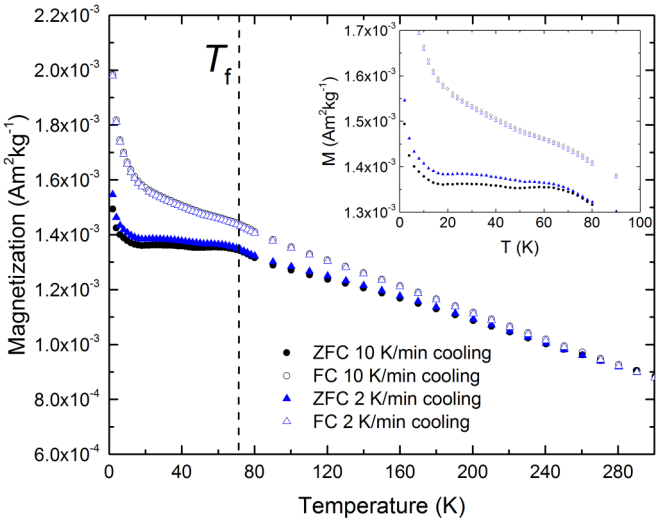

FIG. 1. Magnetization as a function of temperature for LiBN. The sample was cooled at different rates as stated in the legend which highlighted a difference in behavior at low temperatures. *Inset:* enlarged low temperature region of the temperature dependence of the magnetization.

structure and neighboring Li atom. Molecular dynamics [23] and temperature dependent diffraction [24] for the related graphite-alkali compounds show incommensurate alkali layers and alkali ion mobility above 90 K. These graphitic structures order to 2D domained commensurate lattices on cooling. It would be reasonable to assume a similar 2D structure exists here although more work is being done to provide a full structural description. In addition, since each Li atom has an unpaired electron, any exchange mechanism may result in some interesting magnetic behavior, which we demonstrate herein. This chemistry suggests a high temperature region where the lithium ions are mobile and a low temperature range where they are frozen into a distribution whose characteristics will depend on the rate of sample cooling from the mobile to the frozen region. Furthermore, since the sample is underdoped, Li atoms may be isolated or in clusters depending on lattice strain. Powder x-ray diffraction indicates the sample has a similar structure to that of h-BN but with the elongation of the c axis owing to the intercalation of Li atoms. There is also evidence of a metallic Li impurity (<1%).

Magnetization measurements are shown in Fig. 1 where different cooling rates were used to pick apart the glassiness in the magnetism at low temperatures. Zero-field-cooled (ZFC) and field-cooled (FC) data show three distinct regions across the temperature range measured. At the lowest temperatures ($T < 20$ K) the magnetism appears to correlate with paramagentic, Curie-type behavior, from the bulk metallic Li impurity. On warming the magnetization changes slope at approximately 30 K, particularly obvious in the ZFC data as the magnetization appears to plateau. However, there is a clear separation of the curves depending on cooling rate. This type of behavior within the ZFC data is indicative of magnetic glassiness related to an inhomogeneous distribution of magnetic ions or clusters within the sample [25]. At high temperatures ($T > 90$ K) the magnetization decreases linearly, with the ZFC and FC curves

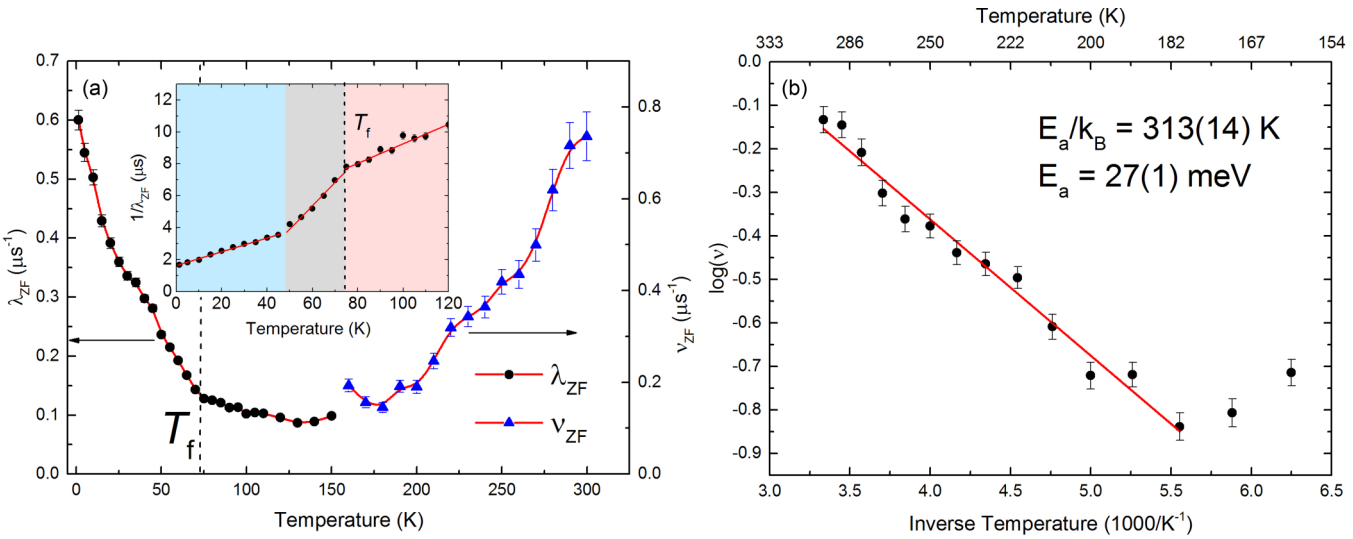

FIG. 2. (a) ZF muon relaxation parameters. *Inset:* the inverse of λ_{ZF}, which shows three discernible regions as well as a clear indication of T_f. (b) Arrhenius plot of the high temperature fluctuation rate from the ZF μSR data.

beginning to merge around 200 K. Above this temperature all curves lie on top of each other, characteristic of a paramagnetic system. Additionally, if one examines the ZFC curves more closely, there is also evidence that the two curves also diverge slightly below 170 K.

It is likely that 70 K, where the two ZFC curves diverge, is a freezing transition, denoted as T_f, since the moment on the Li atoms will be dilute and if randomly distributed will have varying interaction pathways and strengths, a typical behavior for spin glasses. The divergence at 20 K is due to the onset of the Curie tail from paramagnetic Li atoms either trapped in an isolated state or from bulk Li in its metallic form from the disproportionation of the LiBN. Since the system is doped with atomic Li, in order for a ferromagnetic state (glassy or not) to be reached the Li atom positions must be frozen and able to interact. If the Li atoms are mobile at high temperatures, this would involve them freezing into a static state on cooling. The anomalous behavior observed at high temperatures within the magnetic susceptibility measurements may show this. To resolve this ambiguity, μSR measurements have been carried out. This method is sensitive to both nuclear and electronic moments that are static or fluctuating and so separates out the contributions to the magnetism seen in the susceptibility measurements.

Analysis of the μSR data had to be split into two regimes: a high temperature ($T \geqslant 150$ K) and a low temperature ($T \leqslant 150$ K). First, the low temperature region will be discussed, where here the time dependence of the muon polarization or asymmetry [$G(t)$] in ZF was fitted using

$$G(t) = A\left[\exp\left(-\frac{\Delta_{ZF}^2 t^2}{2}\right)\exp(-\lambda_{ZF}t)\right] + A_B, \quad (1)$$

where A is the initial asymmetry from muons stopped in the sample, A_B is the baseline (fixed at 10.9%) arising from muons stopping in the sample holder, Δ_{ZF} is the field distribution from static nuclear moments, and λ_{ZF} is the muon relaxation rate related to the fluctuation rate of the electronic moments. Δ_{ZF} was fixed at 0.29 MHz throughout and calculated in a similar manner to Mansson *et al.* [26], where longitudinal fields are applied to estimate the strength of the nuclear coupling. Figure 2(a) shows the temperature dependence of the muon relaxation rate in ZF. From 150 K down to approximately 75 K λ_{ZF} has a weak T dependence. At 75 K, there is a divergence with a steep rise in the relaxation rate related to a critical slowing down of electronic moments. This is consistent with Li atoms clustering to a magnetic glassy state that is quasistatic with an onset at T_f. Since no precession of the muon spin is observed, this suggests the magnetism to be disordered. There is also a clear paramagnetic component at low temperatures where the fluctuation rate of the paramagnetic moments decreases as the temperature drops and enters the time scale of the μSR experiment. This causes the change in slope around 45 K.

The high temperature region above 150 K was fit using a dynamic Kubo-Toyabe (KT) function [27], which models both the field distribution at the muon site, Δ_{ZF}, and the fluctuation rate, ν, modeling the Li diffusion. Throughout the whole temperature range ($150 < T < 300$ K) Δ_{ZF} was held constant at 0.29 MHz as it is the fluctuating moments that cause changes in the muon relaxation, as opposed to a changing field distribution. The fluctuation rate is shown in Fig. 2(a) for the high temperature region, where there is a clear increase as the temperature increases. From the Arrhenius plot shown in Fig. 2(b), the activation energy, E_a, for this process is 27(1) meV. Transverse field μSR showed similar results, which confirms the sensitivity of the diamagnetic muon to the magnetism and diffusion process within the sample.

To asses whether the Li atoms or the muons are diffusing an NMR experiment was conducted; the high moments of the Li nuclei lend themselves to the NMR technique. At 298 K, the spectrum is typical for a sample where the Li diffuses fast enough to produce NMR "motional narrowing" (see Fig. 3). On cooling, the sharp peak begins to broaden and there is a dramatic loss in amplitude, which is obvious when one integrates the spectra to get the area under the curves [inset of Fig. 3(a)]. We suppose that as the Li mobility increases, its spin-lattice relaxation time decreases as the spectral density at the NMR frequency increases. The NMR data show a similar

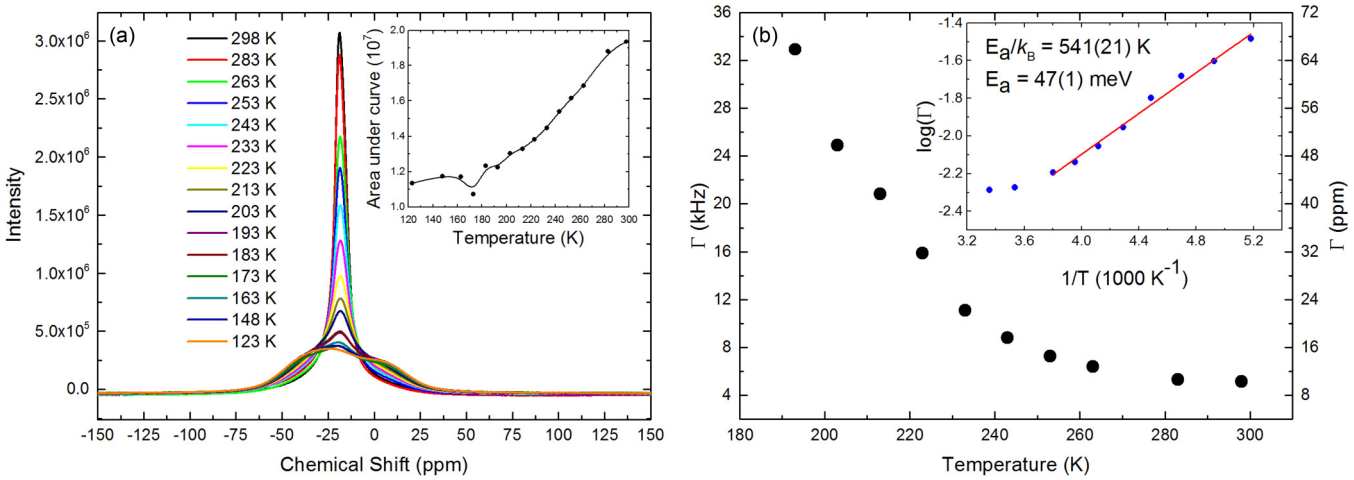

FIG. 3. (a) Chemical shifts of the Li NMR from 298 to 123 K. It is clear from the data that, as the temperature is reduced, structure begins to form in the NMR spectra as the sample goes from the motionally narrowed dynamic state to a static state. *Inset:* integrated area of the curves to illustrate the dramatic changes in the amplitude of the spectra. (b) The FWHM of the NMR spectra as a function of temperature. *Inset:* an Arrhenius plot of the data to give an estimate of the E_a^{NMR}.

relaxation behavior to that of the high temperature data from the μSR data (Fig. 2) and so the two experiments are measuring the same phenomenon.

As mentioned, at high temperatures the NMR response is motionally narrowed and the spectra can be fitted using a Lorentzian peak shape. The full width at half maximum (FWHM, Γ) measures the spin-spin (T_2) relaxation of the Li nuclei and, as for liquids, $T_1 = T_2$.

Figure 3 shows these results where the FWHM has been converted into frequency so one can gauge the time scale of the relaxation. Since this is a measurement of the correlation time of the motions of the Li nuclei, it is clear that as the temperature is lowered the FWHM and thus T_2 increase, indicting a slowing down of the Li diffusion. From an Arrhenius plot $E_a^{NMR} = 47(1)$ meV, which is greater than that derived from the muon data. As already mentioned, the Li atom carries with it an electron, the amount of which could be modulated as the atom hops across the two dimensional lattice. We suggest that the presence of paramagnetism in the high fields needed for NMR may lead to an unrealistic value of E_a^{NMR}. However, the general result that the Li appears to be diffusing above 200 K is valid and of great importance. This allows us to confirm that the muon spin relaxation is due to the diffusion of Li atoms rather than the diffusion of the muon itself.

Since the NMR and μSR experiments all point to the Li atoms diffusing at high temperatures, it is worthwhile to calculate the diffusion constant, D_{Li}, from the μSR data since

$$D_{Li} = \sum_{i=1}^{n} \frac{1}{N_i} Z_{v,i} s_i^2 \nu, \qquad (2)$$

where N_i is the number of Li sites in the ith path, $Z_{v,i}$ is the vacancy fraction, s_i is the jump/hopping distance, and ν is the fluctuation rate, in this case from the muon data. Since the system is in a fairly dilute limit, it is reasonable to assume that the Li atom can jump to any site outlined in Fig. 4 and so the vacancy fraction can be kept constant at 1. The nearest neighbor (first jump) and next-nearest neighbor (second jump) site to which the Li can move are on two different circles with radii of approximately 2.50 Å and 4.32 Å; therefore, one can use these values for Z_{vi}. Since the two sites are equivalent around the circles, N_i can also be fixed at 1 as there is only one equivalent site in both cases for summation. To calculate the jump distances, a cif file created by Kurakevych and Solozhenko [28] was used to get estimates of the bond lengths at 300 K.

The Li diffusion constant was calculated between 150 and 300 K and is shown in Fig. 4. Values of the D_{Li} can vary for different layered Li-intercalated materials depending on the c-axis spacing [29]. In Li-intercalated graphite, measurements of D_{Li} gave values ranging from 10^{-10} cm^2 s^{-1} to 10^{-6} cm^2 s^{-1} at 298 K [30,31]. These values are consistent with those for

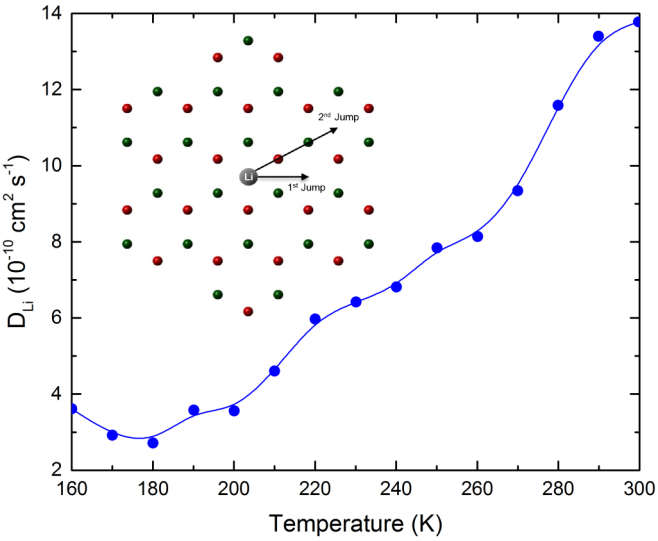

FIG. 4. Diffusion constant from the ZF μSR data using the fluctuation rate (ν) from the dynamic Kubo-Toyabe fits to the data. The inset shows the possible jumps of the Li atom where the first jump corresponds to a distance of ~2.50 Å and the second jump ~4.32 Å.

other Li diffusion constants from μSR experiments [26,32,33]. Given that our system is dilute, there are a large number of vacant sites that the Li can jump to and since the structure is layered, the Li atoms can move freely throughout the structure and so the value of D_{Li} may be reasonable.

From the combination of the dc magnetization and μSR data presented here, there is clear evidence at low temperatures of an emergent magnetic state, albeit glassy. At the highest measured temperatures, we believe that the Li is able to diffuse; this is modeled in the μSR data using the dynamic KT in ZF where the activation energy of 27 meV for the diffusion process is reasonable. NMR also confirms that, above 200 K, one observes the onset of Li diffusion, showing the validity of the muon technique to study this process. There is also a feature in the high temperature region of the magnetization data (Fig. 1) at 200 K, which could indicate the onset of the diffusion of Li atoms and their eventual freezing into a random state. Once the Li atoms become static, they are able to inject both spin and charge partially into the BN layers, where the electronic moment is still fluctuating too fast to be measurable within the time scales of either measurements. However, at 75 K, the electronic moments freeze into a glassy magnetic state, where due to the random Li sites, there are many different exchange interactions within different sized clusters. This causes a glassy ground state to appear but it is clearly shown to be present, even in the absence of an applied external field.

IV. CONCLUSION

To conclude, we have successfully doped atomic Li in the BN structure, which results in a stoichiometry of $Li_{0.01}(BN)_3$. Magnetic measurements have shown some curious features; the likely scenario is that, at high temperatures, the Li atoms are able to diffuse through the layered structure. However, on cooling, the Li atoms freeze into position and correlations between the electronic moments grow to end up in a magnetic ground state. This type of material opens up a new avenue of research and promise, where Li based materials have great use and technological potential in battery materials. BN is a cheap and readily available material and so further research to fully understand the system is needed in order to realize its full effectiveness.

ACKNOWLEDGMENTS

We would like to thank the STFC and the ISIS Neutron and Muon Source for access to the EMU spectrometer as well as measurements within the materials characterization laboratory. We would also like to thank Dr. Paul Smith for assistance with electron spin resonance measurements and Dr. Christopher Blake, Research School of Chemistry, Australian National University for measuring the nuclear magnetic resonance spectra. Special thanks are given to Ruth Bott for reading previous versions of the manuscript.

[1] N. Nitta, F. Wu, J. T. Lee, and G. Yushin, Mater. Today **18**, 252 (2015).
[2] R. Clarke, J. N. Gray, H. Homma, and M. J. Winokur, Phys. Rev. Lett. **47**, 1407 (1981).
[3] A. Lovell, F. Fernandez-Alonso, N. T. Skipper, K. Refson, S. M. Bennington, and S. F. Parker, Phys. Rev. Lett. **101**, 126101 (2008).
[4] K. Watanabe, M. Soma, T. Onishi, and K. Tamaru, Nature **233**, 160 (1971).
[5] M. Hirscher, M. Becher, M. Haluska, U. Dettlaff-Weglikowska, A. Quintel, G. S. Duesberg, Y.-M. Choi, P. Downes, M. Hulman, S. Roth, I. Stepanek, and P. Bernier, Appl. Phys. A **72**, 129 (2001).
[6] M. S. Dresselhaus and G. Dresselhaus, Adv. Phys. **51**, 1 (2002).
[7] I. T. Belash, A. D. Bronnikov, O. V. Zharikov, and A. V. Pal'nichenko, Solid State Commun. **69**, 921 (1989).
[8] J. Kim, E. Yamasue, H. Okumura, K. N. Ishihara, and C. Michioka, J. Alloy Compd. **685**, 135 (2016).
[9] G. L. Doll, J. S. Speck, G. Dresselhaus, M. S. Dresselhaus, K. Nakamura, and S.-I. Tanuma, J. Appl. Phys. **66**, 2554 (1989).
[10] A. Sumiyoshi, H. Hyodo, and K. Kimura, J. Phys. Chem. Solids **71**, 569 (2010).
[11] E. Budak and C. Bozkurt, J. Solid State Chem. **177**, 1768 (2004).
[12] R. Q. Wu, L. Liu, G. W. Peng, and Y. P. Feng, Appl. Phys. Lett. **86**, 122510 (2005).
[13] J. Wu and W. Zhang, Chem. Phys. Lett. **457**, 169 (2008).
[14] J. Yang, D. Kim, J. Hong, and X. Qian, Surf. Sci. **604**, 1603 (2010).
[15] V. Barone and J. E. Peralta, Nano Lett. **8**, 2210 (2008).
[16] Z.-Y. Hu, X. Shao, D. Wang, L.-M. Liu, and J. K. Johnson, J. Chem. Phys. **141**, 084711 (2014).
[17] C.-S. Liu and Z. Zeng, Appl. Phys. Lett. **96**, 123101 (2010).
[18] J. Sugiyama, K. Mukai, Y. Ikedo, H. Nozaki, M. Månsson, and I. Watanabe, Phys. Rev. Lett. **103**, 147601 (2009).
[19] K. Nakamura, H. Ohno, K. Okamura, Y. Michihiro, T. Moriga, I. Nakabayashi, and T. Kanashiro, Solid State Ion. **177**, 821 (2006).
[20] See Supplemental Material at http://link.aps.org/supplemental/10.1103/PhysRevMaterials.1.054405 for information on the synthesis of the LiBN compound.
[21] Results to be published elsewhere.
[22] S. R. Giblin, S. P. Cottrell, P. J. C. King, S. Tomlinson, S. J. S. Jago, L. J. Randall, M. J. Roberts, J. Norrisa, S. Howarth, Q. B. Mutamba, N. J. Rhodes, and F. A. Akeroyd, Nucl. Instrum. Methods, A **751**, 70 (2014).
[23] P. A. Wielopolski and J. W. White, Mol. Phys. **69**, 959 (1990).
[24] G. R. S. Naylor and J. W. White, J. Chem. Soc., Faraday Trans. I **83**, 3447 (1987).
[25] J. A. Mydosh, *Spin Glasses: An Experimental Introduction*, 1st ed. (Taylor and Francis, London, 1993).
[26] M. Månsson, H. Nozaki, J. M. Wikberg, K. Prša, Y. Sassa, M. Dahbi, K. Kamazawa, K. Sedlak, I. Watanabe, and J. Sugiyama, J. Phys.: Conf. Ser. **551**, 012037 (2014).
[27] S. L. Lee, S. H. Kilcoyne, and R. Cywinski, *Muons Science: Muons in Physics, Chemistry and Materials* (Institute of Physics Publishing, London, UK, 2008).
[28] O. O. Kurakevych and V. L. Solozhenko, Acta Crystalogr., C **63**, i80 (2007).
[29] A. van der Ven, J. Bhattacharya, and A. A. Belak, Acc. Chem. Res. **46**, 1216 (2012).

[30] P. Yu, B. N. Popov, J. A. Ritter, and R. E. White, J. Electrochem. Soc. **146**, 8 (1999).

[31] K. Persson, V. A. Sethuraman, L. J. Hardwick, Y. Hinuma, Y. S. Meng, A. van der Ven, V. Srinivasan, R. Kostecki, and G. Ceder, J. Phys. Chem. Lett. **1**, 1176 (2010).

[32] J. Sugiyama, J. Phys. Soc. Jpn. **82**, SA023 (2013).

[33] J. Sugiyama, K. Mukai, H. Nozaki, M. Harada, K. Kamazawa, Y. Ikedo, M. Månnson, O. Ofer, E. J. Ansaldo, J. H. Brewer, K. H. Chow, I. Watanabe, Y. Miyake, and T. Ohzuku, Phys. Proc. **30**, 105 (2012).